Proc. 13th Int. Conf. on Nucleus-Nucleus Collisions
JPS Conf. Proc. **32**, 010063 (2020)
https://doi.org/10.7566/JPSCP.32.010063

Fluorine Nucleosynthesis in AGB stars in the light of the ^{19}F(p,α)^{16}O and the ^{19}F(α,p)^{22}Ne Reaction Rate Measured via the Trojan Horse Method.

S. Palmerini[1,2], G. D'Agata[3], M. La Cognata[4], I. Indelicato[4], R. G. Pizzone[4]

[1]*Dipartimento di Fisica e Geologia, Università degli Studi di Perugia, via A. Pascoli, I-06125 Perugia, Italy*
[2]*I.N.F.N. sezione di Perugia, via A. Pascoli, I-06125 Perugia, Italy*
[3] *Nuclear Physics Institute of the Czech Academy of Sciences, Řež, 25068 Czech Republic*
[4] *I.N.F.N. Laboratori Nazionali del Sud, Via Santa Sofia 62, I-95123, Catania, Italy*

E-mail: sara.palmerini@pg.infn.it

(Received August 3, 2019)

The ^{19}F(α,p)^{22}Ne and the ^{19}F(p,α)^{16}O reactions, namely the two main channels of ^{19}F destruction in stars, have been studied via the Trojan Horse Method (THM) in the energy range typical of the stellar nucleosynthesis. Because of the discovery of resonant structures below 500 keV, the rates of the 2 reactions were found to be larger than before. This fact hints to an enhancements in efficiency of fluorine destruction in stellar H- and He- burning. Since fluorine abundances are observed in their spectra, theAsymptotic Giant Branch (AGB) stars are considered a major source of F for the Galaxy. We re-analyze the fluorine nucleosynthesis in this type of stars, in the light of the new THM reaction rates for ^{19}F destruction.

KEYWORDS: abundances - stars: AGB and post-AGB, nuclear reactions, nucleosynthesis

1. The Fluorine Nucleosynthesis and the AGB Stars

Asymptotic Giant Branch (hereafter AGB) stars, Type II supernovae (SNe II), Wolf-Rayet (W-R) stars as well as Hydrogen-deficient stars formed by white-dwarf merging have been suggested to produce ^{19}F (the sole stable isotope of fluorine) trough different nucleosynthesis processes ([1], [2], [3,4], [5]). Enhanced abundances of F have been observed in a large sample of AGB stars by several authors (see e.g. [6] and references therein). For this reason low mass evolved stars are commonly considered sites for the production of fluorine. Even if there are still doubts whether F yields of AGB stars are sufficient to entirely account for the cosmic fluorine abundance, this hypothesis was foreseen by the findings of [7], whose observations suggest that ν-process in SNe II could not be the main producer of F in the solar neighborhood. Indeed, in the sample of 49 bright K giants studied by the authors, the trends of [F/Fe] versus [Fe/H] and [F/O] versus [O/H] disagree with the typical pattern of the SNII nuclesosynthesis. Since resulting abundance of an isotope (the ^{19}F in our case) can be larger than theoretical predictions because the production channels are more efficient than thought as well as because the destruction mechanisms are less, we investigate the F nucleosynthesis problem by using in our calculations the ^{19}F(p,α)^{16}O and the ^{19}F(α,p)^{22}Ne reaction rates determined via the Trojan Horse Method (hereafter THM).

The AGB phase represents an evolved stage of low mass stars (up to 6-8$M_{\odot}$), during which the thin radiative H-burning shell (placed below the extended and cold convective envelope) provides energy to the star, while the CO stellar core is degenerate. Between the core and the H-shell, there is a He-rich region (the He-shell or intershell) that periodically burns in convective flashes (known

as thermal pulses or *TP*). At the end of each pulse fresh products of the stellar nucleosynthesis are brought to the stellar surface by the *third dredge-up* (hereafter, TDU), a mixing due to the penetration of the convective envelope into the inner stellar layers, which occurs in the few tens of years when the He-burning is exhausted and the H-burning is not resumed yet. In this framework the ^{19}F is produced trough a very complicate network of reactions and it can be also easily destroyed by both proton- and α-captures [8]. Figure 1 shows a scheme of the fluorine nucleosynthesis network along with the temporal evolution of the internal structure of an AGB star. The signature of AGB star nucleosynthesis is the production of nuclei heavier than Fe via the s-processing (or slow neutron captures). It occurs in the He-shell during the TPs thanks to neutrons delivered by the ^{22}Ne(α,n)^{25}Mg reaction and capturing neutrons from the ^{13}C(α,n)^{16}O reaction when the H-shell is burning. The formation of a ^{13}C reservoir just below the H-burning shell plays crucial role for the s-process. It is due to an injection of protons in the stellar layers rich in ^{4}He and ^{12}C, during the TDU, which induces the reaction chain: ^{12}C(p,γ)^{13}N(β)^{13}C. If the amount of injected protons is sufficiently large, also ^{14}N is produced by further proton captures on ^{13}C. Even if the ^{14}N production has to be avoided to guarantee the efficiency of the s-process (because of its very large neutron capture cross section), the ^{14}N is needed to synthesize ^{19}F via the chain ^{14}N(α, γ)^{18}F($\beta^{+}\nu$)^{18}O(p,α)^{15}N(α, γ)^{19}F or the alternative path ^{18}O(p,α)^{15}N(α, γ)^{19}F, in case of proton delivery by the ^{14}N(n, p)^{14}C reaction [9, 10]. Part of the fresh synthesized ^{19}F is later consumed by the ^{19}F(α,p)^{22}Ne during TP. A further destruction of the F

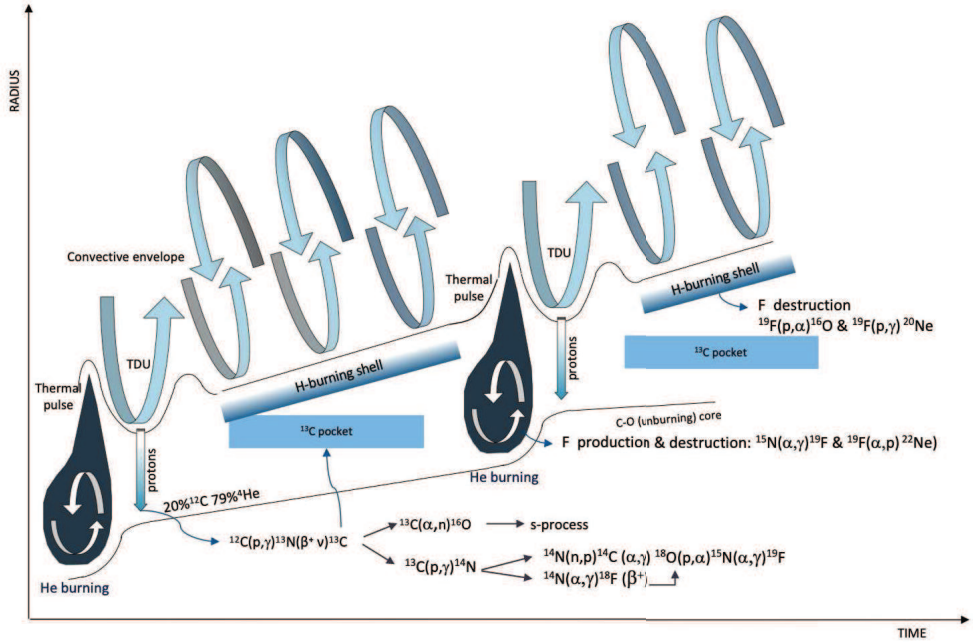

Figure 1. Temporal evolution of the internal structure of an AGB stars. Thermal pulses, the H-burning shell, the He-shell, the ^{13}C-pocket and the convective envelope are indicated by labels as well as the sites of fluorine production and destruction.

occurs in the H-burning shell, where the temperatures are high enough to burn the ^{19}F(p,α)^{16}O and the

^{19}F(p,γ)^{20}Ne reactions, but not the ^{19}F via ^{16}O(p,γ)^{19}F. Furthermore, proton captures at a few $10^7 K$ coupled with non convective exchanging of matter between the border of the convective envelope and the H-burning shell (called extra-mixing [21]) can reduce the surface abundance of fluorine in AGBs of less than 3 $M_\odot$ [11].

2. Measurements of the ^{19}F(p,α)^{16}O and ^{19}F(α,p)^{22}Ne reaction via the Trojan Horse Method

The first experimental data available for the ^{19}F(p,α)^{16}O at astrophysical energies ($E_{c.m.} \leq 300$ keV) were published by the [12]. Until 2011, the widely adopted cross section was the one in the compilation NACRE [13], which use data from different sources to supply a recommended astrophysical factor and reaction rate. The authors observed three resonances in the energy regions of interest applying the THM (see [14] for detail) and determined the cross-section of the two-body ^{19}F(p,α)^{16}O by properly selecting the quasi-free contribution of the three-body reaction ^{2}H(^{19}F, α^{16}O)n (being n the spectator particle and ^{2}H the TH nucleus thanks to its p$\oplus$n cluster structure).

Three experiments [11, 12, 15] confirmed the presence of resonant structures at $E_{cm} \leq 0.6$ MeV and, as a consequence, an enhancement of the reaction rate at astrophysical temperatures (about $10^7 - 10^8 K$), which finally turned out to be increased up to a factor of 1.7 [15]. For a comparison of the reaction rates and details on data analysis we refer to figures 13-16 in [15].

The THM has successfully allowed to investigate also the ^{19}F(α,p)^{22}Ne, whose direct measurements at astrophysical energies (200-1100 keV) are hampered by the Coulomb barrier, 3.1MeV. The lowest energy reached by direct experiment is indeed 660 keV [17] and data are affected by large uncertainties. The ^{19}F(α,p)^{22}Ne was investigate via the THM applied to the ^{19}F(^{6}Li, p^{22}Ne)^{2}H reaction, taking advantage of the well-known cluster structure of the ^{6}Li nucleus ($\alpha \oplus d$). The ^{19}F(α,p)^{22}Ne reaction rate was found to be up to a factor of 4 respect to the direct data available in literature [18,19].

3. Results for AGB star nucleosynthesis

Calculations for F nucleosynthesis for three stellar models of 1.5, 3, and 5 $M_\odot$ and solar metallicity were computed with the NEWTON code [20] (which adopts the pockets of ^{13}C and ^{14}N suggested by [23] and [24], the same cross-sections for neutron captures used by the quoted authors, and the reaction rates of proton and α captures in Table 5 by [19]). The ^{19}F abundances in the He-rich stellar region result smaller in the models computed by adopting the ^{19}F(α,p)^{22}Ne reaction rate determined via THM than in those computed by using the data from [17]. In particular the 5 $M_\odot$ AGB model shows the largest sensitivity to the reaction rate. In this case the ^{19}F abundance in the He-shell estimated by using the THM reaction rate is 4 times smaller that the amount computed with the rate published by [17]. Smaller variations are registered in the 1.5 and 3 $M_\odot$ AGB models, which burn He less efficiently because of the lower temperatures. In any case. The dilution of the nucleosynthesis products with envelope materials due to the TDU makes the effects of the ^{19}F(α,p)^{22}Ne reaction rate on the stellar surface abundances negligible (less than 5%). In the second phase of our analysis the effects of the ^{19}F(p,α)^{16}O reaction in the H-shell was evaluated by computing the composition of the H-burning shell of $2M_\odot$ and solar metallicity AGB stars and running the post-process code MAGIC [21, 25] to estimate the dilution of the surface F abundance due to extra-mixing. (The extra-mixing model we use is the one described in [26]). In figure 2 the fluorine abundance in the envelope of a $2M_\odot$ and solar metallicity AGB (resulting by using the rates of the ^{19}F(p,α)^{16}O reaction [11], [15] and [13]) are compared with the F abundance observed in a sample of AGB stars [6]. All the models show in a quite good agreement with the observations despite the choice made for the ^{19}F(p,α)^{16} cross section. It has to be notice that the differences between the outputs of the nucleosynthesis calculations, due to the different choices of the reaction rates applied, are smaller than the error bars on

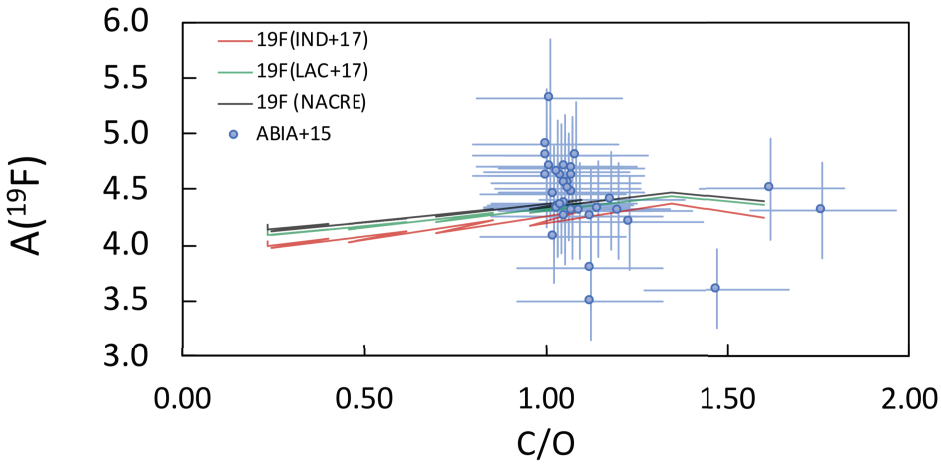

Figure 2. Temporal evolution of the surface abundance of ^{19}F in the $2M_{\odot}$ and solar metallicity AGB model compared with the abundances observed by [6]. Three curves deal with the fluorine abundance profile computed by using the ^{19}F(p,α)^{16}O reaction rate by [13] (black line), [11] (green line) and [15] (red line). The stepwise trend is due to the enrichment in F at each TDU and the F destruction of the extra-mixing during the H-burning periods. The F abundance are reported as a function of the C/O ratio and are in spectroscopic units according with the definition A(^{19}F) = 12 + log(X(^{19}F)/X(H)), being X(H) and X(^{19}F) the abundances by number of H and ^{19}F, respectively.

the stellar data due to the observation uncertainties.

References

[1] S. Cristallo, A. Di Leva, G. Imbriani, et al., **A&A** , 570, 46 (2014).
[2] S. E. Woosley & W. C. Haxton, **Nature**, 334, 45 (1988).
[3] G. Meynet & M. Arnould, **A&A**, 355, 176 (2000).
[4] A. Palacios, M. Arnould, and G. Meynet, **A&A**, 443, 243 (2005).
[5] R. Longland R., P. Lorén-Aguilar, J. José, et al., **ApJL**, 737, 34 (2011).
[6] C. Abia C., K. Cunha, S. Cristallo, et al., **A&A**, 581, 88 (2015).
[7] H. Jonsson, N. Ryde, E. Spitoni, et al., **ApJ** , 835, 50 (2017).
[8] M. Lugaro, C. Ugalde, A.I. Karakas, et al., **ApJ**, 615, 934 (2004).
[9] S. Cristallo, O. Straniero, R. Gallino, et al., **ApJ**, 696, 797 8 (2009).
[10] M. Forestini, S. Goriely, A. Jorissen, and M. Arnould, **A&A**, 261, 157 (1992).
[11] M. La Cognata, S. Palmerini, C. Spitaleri, et al., **ApJ**, 805, 128 (2015).
[12] M. La Cognata, A. M. Mukhamedzhanov, C. Spitaleri, et al. **ApJL**, 739, 54 (2011).
[13] C. Angulo, M. Arnould, M. Rayet, et al., **NuPhA**, 656, 3 (1999).
[14] C. Spitaleri, M. La Cognata, L.Lamia L., et al., **EPJA**, 52, 77 (2016).
[15] I. Indelicato, M. La Cognata, C. Spitaleri, et al., **ApJ**, 845 19 (2017).
[16] I. Lombardo I., D. Dell'Aquila, A. Di Leva, et al., **PhLB**, 748, 178 (2015).
[17] C. Ugalde, R.E. Azuma, A. Couture, et al., **PhRvC**, 77, 035801 (2008).
[18] R.G. Pizzone, G. D'Agata, M. La Cognata, et al., **ApJ**, 836, 57 (2017).
[19] G. D'Agata, R.G. Pizzone, M. La Cognata, et al., **ApJ** , 860, 61 (1992).
[20] O.Trippella, M. Busso M., E. Maiorca, et al., **ApJ**, 787, 41 (2014).
[21] S. Palmerini, M. La Cognata, S. Cristallo, and M. Busso, **ApJ**, 729, 3 (2011).
[22] I.J. Sackmann & A.I. Boothroyd, **ApJ**, 392, L71 (1992).
[23] O. Trippella, M. Busso, S. Palmerini, et al., **ApJ**, 818, 125 (2016).
[24] S. Palmerini, O. Trippella, M. Busso, et al., **Ge.Co.A.**, 221, 21 (2018).
[25] S. Palmerini, S. Cristallo, M. Busso, et al., **ApJ**, 741, 26 (2011).
[26] S. Palmerini, O. Trippella, M. Busso, **MNRAS**, 467, 1193 (2017).